Wnt Pathway Activation by Placental Mesenchymal Stem Cells Promotes Hepatic Regeneration in a Cirrhotic Rat Model

Jong Ho Choi
Gangneung-Wonju National University College of Dentistry
Ji Hye Jun
CHA University - Pocheon Campus: CHA University
Gi Dae Kim
Kyungnam University
Eek-hoon Jho
University of Seoul
Soon Koo Baik
Yonsei University Wonju Christian Hospital: Wonju Severance Christian Hospital
Si Hyun Bae
Catholic University of Korea College of Medicine: Catholic University of Korea School of Medicine
Gi Jin Kim (gjkim@cha.ac.kr)
CHA University https://orcid.org/0000-0002-2320-7157

Research

Keywords: placenta-derived mesenchymal stem cells, liver regeneration, vascular niche, Wnt signaling

Posted Date: September 2nd, 2021

DOI: https://doi.org/10.21203/rs.3.rs-850530/v1

Abstract

Background: Sinusoidal endothelial cells (SECs) in liver play important roles in hepatocyte regeneration. We recently reported placenta-derived mesenchymal stem cells (PD-MSCs) can promote hepatic regeneration in a damaged liver model *via* dynamic events. However, the effects of PD-MSCs on vascular structure in liver tissues remain unknown. We therefore investigated alteration of vascular structure and function in carbon tetrachloride (CCl_4)-injured rat model following transplantation (Tx) with PD-MSCs.

Methods: PD-MSCs were engrafted into CCl_4-injured rat model via intravenous Tx. Expression markers related to angiogenic factors and Wnt signaling pathway were analyzed by quantitative real time-PCR, Western blot, and immunofluorescence *in vitro* and *in vivo*. Furthermore, endothelial permeability assay was performed to confirm the effect of PD-MSCs on the functional regeneration of injured endothelial cells *in vitro* co-culture system.

Results: PD-MSCs were found to significantly reduce the expanded hepatic vein diameter and increased tube formation of the aorta in both *in vitro* and *ex vivo* co-culture systems. PD-MSCs also increased the expression of angiogenic factors and activated the Wnt signaling pathway. Furthermore, PD-MSCs reduced endothelial permeability *via* activation of β-catenin in the *in vitro* co-culture system.

Conclusions: Taken together, PD-MSCs transplantation (PD-MSC Tx) improves the structure and function of SECs by activating Wnt signaling, which triggers hepatic regeneration, in a CCl_4-injured rat model. Therefore, these findings suggest that vascular restoration induced by PD-MSCs supports liver regeneration in a hepatic failure model and can be applied as a cell-based therapy.

Background

Liver cirrhosis is closely related to difficult-to-treat liver diseases and is associated with high mortality and morbidity. In the cirrhotic state, irreversible biophysical changes, such as excessive apoptosis of hepatocytes and accumulated collagen deposition by activated hepatic stellate cells, appear in the liver microenvironment [1]. Furthermore, these biophysical changes destroy normal tissue in the liver (e.g., vascular structure and its composition). Generally, hepatic vascular structures in the liver tissues play critical roles in providing blood to hepatocytes during liver regeneration [2]. Liver sinusoidal endothelial cells (LSECs) are involved in liver regeneration *via* vascular proliferation and the regulation of endothelial permeability *via* the interaction with several microenvironmental factors such as nitric oxide (NO). Of note, alteration of the LSEC phenotype from differentiated to capillarized is also critical for the development of cirrhosis mediated by activated hepatic stellate cells as well as the proliferation of hepatocytes after damage [2]. A previous study reported that the release of vascular endothelial growth factor (VEGF) from endothelial cells induced hepatocyte proliferation during liver regeneration by activating nuclear factor-kappa B (NF-κB), hepatocyte growth factors (HGF) and EC-specific transcription factor Id1 [3].

However, Rodriguez-Vilarrupla A et al. reported that activation of PPARα improves endothelial dysfunction and reduces fibrosis by increasing NO bioavailability in cirrhotic rats [4]. Therefore, many studies examining the underlying mechanisms of endothelial cell physiology in liver tissue during liver regeneration and cirrhosis are actively underway. Nevertheless, although there has been increasing interest in the role of hepatic vessels in liver cirrhosis, therapeutic mechanisms and factors involved in liver regeneration induced by vascular function are poorly understood.

β-Catenin is a key regulator of homeostasis in several tissues and regulates the Wnt signaling pathway *via* transcriptional activity [5]. Some studies reported that inhibition of Wnt signaling in the liver leads to metabolic disability and pathophysiological events [6]. β-Catenin-dependent Wnt signaling is essential for endothelial cell survival and proliferation. β-Catenin is also known as a regulator of endothelial permeability [7]. In particular, paracellular pathway-mediated endothelial permeability is regulated by endothelial cell-cell junctions involving adhesion molecule VE-cadherin. β-Catenin and VE-cadherin are major components of functional adherent junctions. VEGF also regulates endothelial integrity and permeability by modulating the VE-cadherin and β-catenin interaction [8, 9]. In addition, Frizzled (Fz)/low-density lipoprotein receptor-related proteins 5 and 6 (LRP5 and LRP6), which are upstream factors of β-catenin, are critical regulators of the Wnt/β-catenin signaling cascade in the vasculature [10]. Recently, there has been increasing interest in the role of Wnt/β-catenin signaling in the pathology of ovarian, myocardial, and neuronal diseases [11, 12]. Previous studies have demonstrated that disruption of endothelial β-catenin signaling affects endothelial tight junctions in tissues, resulting in loss of vascular integrity and nerve and cardiac injury [13]. Although researchers have suggested that Wnt/β-catenin signaling is associated with liver fibrosis [14], no study has determined whether β-catenin controls vascular remodeling in the liver cirrhosis model.

Mesenchymal stem cells (MSCs) have been studied for their capacity to facilitate liver regeneration in severe liver injuries and their utility as cell sources for degenerative disease [15]. Transplanted MSCs have been shown to migrate into damaged tissues in response to chemotactic signals released during inflammation [16]. Recently, co-culturing MSCs and human umbilical vein endothelial cells (HUVECs) was shown to upregulate Wnt/β-catenin signaling, as detected by nuclear localization of β-catenin [17]. Furthermore, the MSC-endothelial cell interaction induced the expression of VE-cadherin and β-catenin, and MSCs were found to modulate vascular permeability in acute lung injury [18, 19]. Recently, we reported that PD-MSCs have the capacity to differentiate into hepatocytes and have a therapeutic effect in CCl_4-injured rat liver through anti-fibrotic and autophagic mechanisms [20, 21]. We also observed that microenvironmental factors, niches, including hypoxia, adhesion molecules (e.g., integrin α4 and Rho signaling), and endothelial cells induced increases in PD-MSC migration activity using an *in vitro* co-culture system [22]. However, there has been little discussion about the effect of MSCs on vascular remodeling and hepatic regeneration in the liver cirrhosis model.

Therefore, in this study we investigated whether PD-MSCs regulate alterations in vascular structure and functional improvement of the endothelium, including permeability, in a CCl_4-injured rat model.

Furthermore, we investigated whether vascular remodeling *via* PD-MSC-mediated Wnt signaling improves hepatic regeneration in a CCl_4-injured cirrhotic rat model.

Methods

Human liver specimen

Human liver tissues from normal and cirrhotic patients were provided by Yonsei University, Wonju College of Medicine (Korea-21 Cirrhosis Project). All participants provided written informed consent prior to sample collection. Ultrasound-assisted liver biopsy was performed with a 16-gauge needle and 15 mm biopsy specimen notch. Biopsy samples were selected by thickness of the predominant septa type, and small nodules were selected for scoring. The degree of fibrosis and cirrhosis in biopsied specimens was evaluated according to the Laennec system, such as no definite fibrosis (n=5), minimal fibrosis (n=5) and severe cirrhosis (n=5).

CCl_4-injured rat liver model

Six-week-old Sprague-Dawley rats were purchased (Orient Bio Inc., Seongnam, Korea) and maintained in an air-conditioned animal facility. Liver cirrhosis was induced by intraperitoneal (i.p.) injection of CCl_4 (approximately 1.6 g/kg; Sigma-Aldrich, St. Louis, MO, USA) dissolved in corn oil to a concentration of 0.8 mg/ml and injected at 0.2 ml/100 g body weight twice a week for 9 weeks. An equal volume of corn oil was injected into control animal (n=5), and animals in the negative control group (CCl_4; n=5) were sacrificed after CCl_4 treatment for 9 weeks. PD-MSCs ($2x10^6$ cells) were transplanted by intrasplenic transplantation (PD-MSC Tx, n=19), and NTx rats were maintained as sham controls (n=19). Liver tissues were harvested at 1, 2 and 3 weeks from rats in all groups. All animal experimental processes were conducted using protocols according to the Institutional Review Board of CHA General Hospital, Seongnam, Korea (IACUC-130009).

Cell culture

Placenta collection and their use for research were approved by the Institutional Review Board of CHA General Hospital, Seoul, Korea (IRB #07-18). PD-MSCs were isolated as previously described [21]. Briefly, the chorionic membrane was separated from the placenta. Then, cells were scraped from the membrane and digested with 0.5% collagenase IV (Sigma-Aldrich) for 40 minutes at 37℃. Harvested cells were cultured in Ham's F-12/DMEM supplemented with 10% fetal bovine serum (FBS), 100 U/ml penicillin and 100 μg/ml streptomycin (Gibco-Invitrogen, Grand Island, NY, USA) for stabilization. PD-MSCs were cultured in α-MEM (Gibco-Invitrogen) supplemented with 10% FBS, 100 U/ml penicillin, 100 μg/ml streptomycin (Gibco-Invitrogen), 100 μg/ml heparin (Sigma-Aldrich), and 25 ng/ml FGF4 (PeproTech, Inc., Rocky Hill, NJ, USA) at 37℃ in a 5% CO_2 incubator.

Histopathological analysis

Liver tissues were fixed in 10% buffered formaldehyde (MERCK, Kenilworth, NJ, USA), embedded in paraffin, and sectioned to a thickness of 5 μm. Tissue sections were stained with hematoxylin and eosin (H&E). Portal vein diameter was quantified with image processing software (ImageJ, NIH).

Immunostaining

To analyze the localization of active β-catenin in liver, sections from paraffin-embedded tissues were stained with anti-active β-catenin antibody (Cell Signaling) at 4℃ overnight and then incubated with biotinylated IgG at room temperature for 1 hour. Sections were then incubated with 3,3'-diaminobenzidine (DAB), and images were captured with an Axioplan 2 microscope (Carl Zeiss, Thornwood, NY, USA).

To analyze the localization of markers related to human-specific antibodies (Stem121: human cytoplasmic marker and human nuclei) and antibodies for angiogenic markers and active β-catenin, liver samples were embedded in Tissue-Tek OCT Compound (Sakura Finetechnical Co. Ltd, Chuo-ku, Tokyo, Japan) and stored at -80℃. Cryostat sections (7 μm thick) were fixed in 100% methanol (MERCK) and then incubated in 5% BSA for 30 minutes at room temperature. Mouse anti-Stem121 and anti-human nuclei antibodies were used as primary antibodies to detect engrafted PD-MSCs in tissues; samples were incubated with these antibodies at 4℃ overnight and were then incubated with an Alexa 488 (1:200 dilution; Invitrogen)-conjugated secondary antibody at room temperature for 1 hour. To detect the localization between vWF and active β-catenin in liver tissue, samples were incubated with the primary antibodies, rabbit anti-vWF and anti-active β-catenin antibodies, at 4℃ overnight, followed by incubation with an Alexa 488 and 569 (1:200 dilution; Invitrogen)-conjugated secondary antibody at room temperature for 1 hour. DAPI (Invitrogen) staining was used as a counterstain. Images were detected using a Zeiss Axioskop2 MAT microscope (Carl Zeiss MicroImaging).

Real-time PCR

Total RNA was isolated from human liver tissues and cells using TRIzol (Invitrogen). The RNA concentration was measured at 260nm using a spectrophotometer. Reverse transcription was performed with 500ng of total RNA and Superscript III reverse transcriptase (Invitrogen). cDNA were amplified by PCR. Real-time PCR was performed using SYBR EX taq (Roche) and Exicycler TM96 quantitative thermal block (Bioneer). PCR reaction conditions was as follows: denaturation 95℃ for 15minutes and 20 seconds, followed by 40 cycles of 95℃ for 30sec. Annealing 52~60 ℃ for 40 seconds. Extension at 70℃ for 15min. final extension at 72℃ for 7min. Gene expression was normalized to that of an 18s RNA. The sequences of the primers: human β-catenin (NM_001098209.1) forward 5'- AGC CTG TTC CCC TGA GGG TAT TTG-3', human β-catenin reverse 5'- GAC TTG GGA GGT ATC CAC ATC CTC-3', human LRP-6 (NM_002336.2) forward 5'- CAG GGT GGA ATG AAT GTG C-3', human LRP-6 forward 5'- GTG GAT GGG AAG GAT GAT G-3', human GSK-3β (NM_001146156.1) forward 5'- GGA ACT CCA ACA AGG GAG CA-3', human GSK-3β reverse 5'- TTC GGG GTC GGA AGA CCT TA-3', human *Axin2* (NM_004655.3) forward 5'- TCC CCA CCT TGA ATG AAG AA-3', human *Axin2* reverse 5'- TGG TGG CTG GTG CAA AGA-3', human 18s RNA (NR_003286.2) forward 5'- GTA ACC CGT TGA ACC CCA TT-3', human 18s RNA reverse 5'- CCA TCC AAT CGG TAG TAG CG-3'. All reactions were performed in triplicate.

Liver tissue from CP-MSCs transplanted rats were homogenized, DNA was extracted with phenol/chloroform (Invitrogen) and precipitated with ethanol, and total DNA was assayed by UV absorbance. Real-time PCR assay was performed with 300ng of target DNA, Alu-specific primers, and a fluorescent probe (PMID: 12745583) by using Exicycler TM96 quantitative thermal block (Bioneer). Gene expression was normalized to that of a rat GAPDH. The sequences of the primers: human Alu forward 5'-CTG GGC GAC AGA ACG AGA TTC TAT-3', human Alu reverse 5'- CTC ACT ACT TGG TGA CAG GTT CA-3', rat GAPDH (NM_017008.4) forward 5'- GGA AAG CTG TGG CGT GAT-3', rat GAPDH reverse 5'- AAG GTG GAA GAA TGG GAG TT-3'. All reactions were performed in triplicate.

Western blot analysis

Liver tissues from rat model in each group and co-cultured cells were homogenized and lysed in protein lysis buffer (Sigma-Aldrich) supplemented with phosphatase inhibitor cocktail II (A.G scientific) and Complete mini protease inhibitor cocktail (Roche). Equal amounts of protein from each group were pooled. The protein lysates were loaded onto 10-12% SDS-PAGE gel, and the separated protein were transferred to PVDF membranes (BIO-RAD), blocked with 5% bovine serum albumin (BSA) diluted by wash buffer and then incubated overnight at 4℃ with one of the following primary antibodies as indicated: mouse anti-Albumin (1:500, Santa Cruz), rabbit anti-HIF-1α (1:1,000, Seoul University), rabbit anti-vWF (1:1,000, Santa Cruz), goat anti-Endoglin (1:1,000, R&D system), mouse anti-VEGF (1:1,000, R&D system), rabbit anti-VE cadherin (1:500, Cell signaling), rabbit anti-β-catenin (Active form; 1:500, Cell signaling), rabbit anti-phosphorylated LRP-6 (1:1,000, Cell signaling), rabbit anti-GAPDH (1:3,000 Abcam). Membranes were washed and then incubated with a secondary antibody (horseradish peroxidase conjugated anti-mouse IgG (1:5000, Bio-Rad Laboratories) or anti-rabbit IgG (1:10,000, Cell Signaling) or anti-goat IgG (1:5000, Santa Cruz Biotechnology) for 1hrs at room temperature. After washing, the membranes were reacted using an enhanced chemiluminexcence reagent (Pierce).

In vitro co-culture system using the transwell system

To detect Wnt signaling in the *in vitro* model, WB-F344 cells ($6x10^4$ cells) and HUVECs ($2x10^4$ cells) were seeded onto cover glasses (Marienfeld GmbH & Co., Huntington Beach, CA, USA) in a 6-well culture plate (BD Falcon, Franklin Lakes, NJ, USA), and then WB-F344 cells and HUVECs at 80% confluence were exposed to 3 mM CCl_4 for 24 hours. The next day, WB-F344 cells and HUVECs were respectively treated with the Wnt inhibitors BIO (10 nM) and IWP-2 (54 nM) (Stemgent Co., Lexington, MA, USA) and co-cultured with transwell inserts containing PD-MSCs ($2x10^4$ cells).

Endothelial permeability assay

HUVECs ($4x10^4$ cells/well) were seeded into the upper chambers of 24-well transwell plates and cultured for 2 days to allow growth of a confluent monolayer. Monolayers were treated with 3 mM of CCl_4 or Wnt inhibitors (10 nM of BIO and 54 nM of IWP-2, Stemgent Inc., MA, USA). After 24 hours, HUVECs monolayers treated with or without IWP-2 (54 nM) were co-cultured with PD-MSCs ($4x10^4$ cells/well) for

24 hours to inhibit endogenous expression of Wnt-related proteins in PD-MSCs. Endothelial permeability was tested by adding 10 µl of 10 mg/mL fluorescein isothiocyanate (FITC)-dextran (Sigma-Aldrich) to the upper transwell chamber for 30 minutes. After 30 minutes, 100 µl of conditioned medium in the lower chamber was transferred to a 96-well plate (BD Falcon), and the FITC signal was detected at excitation and emission wavelengths of 490 and 525 nm, respectively, for 1 hour. Experiments were performed in triplicate.

Statistical analysis

Statistical significance was evaluated using Student's *t*-test with a significance level of $p<0.05$, and data are presented as the mean ± standard deviation (SD). Data were analyzed using ANOVA. Specific contrast analysis was performed using an LSD post hoc test. All statistical analyses were performed using SAS software (ver. 9.1; SAS institute. Cary, NC, USA).

Results

Engrafted PD-MSC decreases the hepatic vein diameter and improves the liver regeneration in the CCl_4-injured rat model

Engrafted PD-MSCs were detected in CCl_4-injured liver tissues of the PD-MSC transplantation (PD-MSC Tx) group by immunofluorescent staining of a human-specific cytoplasmic marker Stem121. The expression of vWF was detected in hepatic vessels of the control group but not in the NTx group. Interestingly, engrafted PD-MSCs were distributed around the hepatic vein, and vWF expression was higher in the PD-MSC Tx group than in the NTx group (Fig. 1A). In addition, the expression level of human Alu mRNA was significantly elevated in the PD-MSC Tx group compared to that in the non-transplantation (NTx) groups at 1 and 2 weeks; however, the expression was considerably reduced by 3 weeks ($p < 0.05$) (Fig. 1B).

Compared to those in the control group, CCl_4-injured livers in the NTx groups showed severe cirrhosis and increased inflammatory cell infiltration and localization around hepatic vessels. Interestingly, compared to that in the NTx group, the level of cirrhosis in the Tx group was visibly reduced (Fig. 1C). In addition, we investigated whether hepatic vein structures were changed by CCl_4-induced liver damage. In general, it is well known that portal hypertension is increased in cirrhotic liver *via* portal vein thrombosis [23, 24]. As shown in Fig. 1C, the hepatic vein diameter was considerably larger in the CCl_4-treated group than in the control group. Furthermore, the diameter of the hepatic vein gradually widened in a time-dependent manner (1, 2 and 3 weeks). However, the hepatic vein diameter was significantly smaller in the PD-MSC Tx group than in the NTx groups at 1, 2 and 3 weeks (Fig. 1D, $p < 0.05$). Furthermore, the structure of hepatic vessels in the PD-MSC Tx groups were similar to that in the control group, whereas the NTx group showed a very irregular structure of hepatic vessels at 1, 2 and 3 weeks (Supplementary Fig. 2).

Furthermore, we investigated the expression levels of proteins related to hepatic markers, such as albumin (ALB) and hypoxia-inducible factor-1alpha (HIF-1α) to confirm the effect of PD-MSCs on hepatic regeneration in the CCl_4-injured rat model. The expression level of ALB at 1, 2 and 3 weeks was significantly lower in the NTx groups than in the control group. However, the expression level of ALB at 1 and 2 weeks was significantly increased in the PD-MSC Tx group compared with that in the NTx group, but there was no significant difference in ALB expression at 3 weeks between the groups ($p < 0.05$) (Fig. 1E). Compared to the levels in the control group, HIF-1α levels remained decreased up to 3 weeks after injection of CCl_4. Interestingly, the expression levels of HIF-1α at 1, 2 and 3 weeks were significantly higher in the PD-MSC Tx group than those in the NTx group ($p < 0.05$) (Fig. 1F). In our previous reports, increased HIF-1α expression by PD-MSC Tx triggered liver regeneration *via* an autophagic mechanism [20]. Based on these data, we hypothesized that increased HIF-1α expression, mediated by PD-MSC Tx, could increase VEGF expression, which is a downstream factor of HIF-1α. These results suggest that engrafted PD-MSC promotes the recovery of expanded hepatic vein and regeneration in the CCl_4- injured rat model.

PD-MSCs induce angiogenesis and tube formation of endothelial cells in both in vivo and ex vivo co-culture systems

To confirm the effect of PD-MSCs on hepatic angiogenesis, we determined the protein expression profiles of angiogenic markers such as vWF, endoglin, VEGF and VE-cadherin. The expression levels of vWF and endoglin were decreased up to 3 weeks after CCl_4 injection compared to the expression levels in the control group. However, the levels of vWF and endoglin at 1 week were significantly higher in the PD-MSC Tx group than in the NTx group ($p < 0.05$) (Fig. 2A and B). Additionally, at 1 and 2 weeks, the levels of VEGF, which is a key factor in generating new blood vessels after injury, were significantly higher in the PD-MSC Tx group than in the NTx group ($p < 0.05$) (Fig. 2D). In general, VE-cadherin regulates blood vessel formation by modulating VEGF receptor in endothelial cells [25]. Therefore, we confirmed the protein expression of VE-cadherin in the CCl_4-injured rat model. Compared to the expression levels in the control group, the expression level of VE-cadherin at 1, 2 and 3 weeks was suppressed after CCl_4 injection. However, VE-cadherin expression levels at 1, 2 and 3 weeks were dramatically higher when PD-MSCs were transplanted (PD-MSC Tx group) than when these cells were not transplanted (NTx group) ($p < 0.05$) (Fig. 2E). These results suggest that PD-MSCs promote restoration of pathophysiological blood vessels in CCl_4-injured rats through various angiogenic factors including VE-cadherin. In addition, these data suggest that vessels restored by PD-MSC Tx are involved in hepatic regeneration, with these vessels modulating the microenvironment in injured liver tissues.

Next, using a modified aortic ring assay, we confirmed whether PD-MSCs promote hepatic regeneration by upregulating new vessel formation *ex vivo*. In the tube formation assay using aortic samples, the length of branch outgrowth from the aorta was significantly decreased by treatment with CCl_4 in the absence of PD-MSC co-culturing (Co-free group) compared to control culture conditions ($p < 0.05$) (Fig. 2C and F). In addition, the number of 5-bromo-2'-deoxyuridine (BrdU)-positive hepatocytes was significantly decreased

by CCl_4 treatment only but not control treatment conditions ($p < 0.05$) (Fig. 2C and G). However, tube formation was significantly recovered by co-culture with PD-MSCs compared to CCl_4 treatment only ($p < 0.05$). Additionally, hepatocyte proliferation was significantly higher in the PD-MSC co-culture group than in the CCl_4 treatment only group ($p < 0.05$) (Fig. 2C and G). Furthermore, hepatocyte proliferation with vessel recovery by PD-MSCs was similarly observed in the *in vitro* co-culture system (Supplementary Fig. 3). These results suggest that engrafting PD-MSCs into a damaged liver promotes hepatocyte proliferation by inducing the formation of new vessels with adjacent hepatic vein in the CCl_4-injured rat model.

PD-MSC Tx increases the expression and nuclear translocation of β-catenin in CCl_4-injured rats

The Wnt signaling pathway is known to regulate angiogenesis of endothelial cells. Specifically, Wnt and β-catenin regulate the formation of capillary-like networks and endothelial cell proliferation [26]. Therefore, we investigated whether PD-MSCs promote Wnt/β-catenin signaling in CCl_4-injured rat liver. Axin2 regulates the transcriptional activity of Wnt/β-catenin signaling [27]. The expression level of Axin2 mRNA was higher in the CCl_4-damaged liver group, including the NTx group, than in the control group. However, Axin2 mRNA expression level at 1 week was significantly higher in the PD-MSC Tx group than in the NTx group ($p < 0.05$) (Fig. 3A). Also, we evaluated the protein expression of p-LRP6, which is a known upstream regulator of β-catenin, in CCl_4-injured liver, and we found that p-LRP6 protein levels were reduced after CCl_4 injection. However, at 1 and 2 weeks, the levels of p-LRP6 in the PD-MSC Tx group were significantly higher than those in the NTx group ($p < 0.05$) (Fig. 3B). Similarly, the protein expression of active β-catenin (β-catenin) at 1, 2 and 3 weeks was reduced in the CCl_4-treated and NTx groups. However, the expression of β-catenin at 1 week was dramatically higher in the PD-MSC Tx group than in the NTx group, although there were no significance differences in its expression at 2 and 3 weeks between the two groups ($p < 0.05$) (Fig. 3C).

To confirm whether PD-MSC Tx-induced upregulation of β-catenin is specifically detected in the hepatic endothelium, we performed immunofluorescence in CCl_4-injured rat liver using anti-β-catenin antibody. β-Catenin was localized in the nucleus of hepatic endothelial cells (arrow indicates active β-catenin in endothelial cells) or in the hepatocyte transmembrane, but vWF was only localized in hepatic vessels in the control liver (Fig. 3D). In addition, β-catenin was expressed in only the hepatic endothelium, and its translocation from the cytoplasm to the nucleus was reduced in hepatic endothelial cells in the NTx liver. In contrast, there was a striking increase in β-catenin expression in the nucleus of hepatic endothelial cells, and it was co-localized with vWF in the PD-MSC Tx group but not in the NTx group (Fig. 3D). Thus, through upregulation of Axin2 and pLRP6, PD-MSCs have been suggested to promote β-catenin stabilization by upregulating the expression and translocation of β-catenin into the nucleus of hepatic endothelial cells in CCl_4-injured rats.

Wnt pathway gene expression was decreased in human cirrhotic liver

To examine the correlation between liver cirrhosis and the Wnt signaling pathway, we investigated the expression of Wnt signaling-related genes and protein localization in cirrhotic human liver. The localization pattern of β-catenin in human cirrhotic liver was similar to that of the animal model. Interestingly, β-catenin expression was gradually decreased in human liver in a stage-dependent manner (Fig. 4B and G). However, β-catenin was translocated from the cytoplasm to the nucleus in endothelial cells from stage I cirrhotic liver compared to that from stage 0 liver (Fig. 4G). LRP6 mRNA level was also significantly lower in stage III cirrhotic liver than in stage 0 ($p < 0.05$) and stage I livers ($p < 0.05$) (Fig. 4A). However, expression of GSK3β, which is a negative regulator of β-catenin signaling, gradually increased in stage III cirrhotic liver compared to stage 0 ($p < 0.05$) and stage I ($p < 0.05$) (Fig. 4C). Axin2 expression was significantly higher in stage I cirrhotic liver than in stage 0 liver, but there was no significant difference in stage III cirrhotic liver ($p < 0.05$) (Fig. 4D). Interestingly, expression levels of c-Myc and cyclin D1, which are transcriptional factors mediated by β-catenin in endothelial cells, were significantly lower in stage III cirrhotic liver than in stage 0 and stage I livers ($p < 0.05$) (Fig. 4E and F). Based on these results, we hypothesized that the Wnt signaling pathway could be involved in liver cirrhosis or liver regeneration.

Effect of co-culturing PD-MSCs with CCl_4-treated HUVECs and rat hepatocytes on Wnt signaling in the in vitro co-culture system

To confirm the effect of co-culturing PD-MSCs with HUVECs and WB-F344 cells on the expression of Wnt signaling markers *in vitro*, we introduced Wnt inhibitors (BIO: GSK3β inhibitor, IWP: LRP6 inhibitor) into the co-culture system. First, we established 10 nM BIO and 54 nM IWP-2 as optimal concentrations that elicited upregulation or downregulation of β-catenin in the treated group compared to untreated control ($p < 0.05$) (Supplementary Fig. 4). Protein expression levels of β-catenin and p-LRP6 were significantly higher in the BIO-treated group than in the untreated control group ($p < 0.05$). In contrast, β-catenin and p-LRP6 protein expression levels in the CCl_4-treated group were significantly lower than the levels in the control group ($p < 0.05$). Furthermore, compared with Co-free conditions, PD-MSC co-culturing significantly increased the expression of β-catenin and p-LRP6 regardless of BIO or CCl_4 treatment ($p < 0.05$) (Fig. 5A and B). In contrast, the expression levels of active β-catenin and p-LRP6 were effectively inhibited by IWP-2 treatment in both the control and CCl_4-treated groups ($p < 0.05$) (Supplementary Fig. 4). However, decreased β-catenin and p-LRP6 expression levels in directly co-cultured cells (HUVECs and WB-F344 cells) were significantly increased by PD-MSC co-culturing regardless of BIO or CCl_4 treatment ($p < 0.05$) (Supplementary Fig. 4).

In addition, β-catenin localization was detected in the transmembrane of rat hepatocytes or the nucleus of HUVECs in the control group, but these localizations were not detected following CCl_4 treatment. However, β-catenin localization was rescued when both cell types were co-cultured with PD-MSCs regardless of BIO or CCl_4 treatment (Fig. 5C). These results showed that PD-MSCs promote hepatic regeneration in cirrhotic liver *via* hepatic angiogenesis by activating the β-catenin-mediated Wnt pathway.

PD-MSCs effectively decrease HUVEC permeability through the Wnt pathway in the in vitro co-culture system

To investigate whether PD-MSCs promote endothelial cell permeability through the Wnt pathway, we adopted the endothelial permeability assay (Fig. 6A). Endothelial permeability was significantly blocked by BIO treatment compared to control group ($p < 0.05$). However, although permeability was significantly increased by damaging cells with CCl_4 treatment but not by control conditions ($p < 0.05$), there was no significant difference between BIO and CCl_4 treatment. In addition, endothelial permeability was strongly inhibited by PD-MSC co-culturing in the CCl_4-treated group and in the combined BIO and CCl_4-treated group, even though there was no synergistic effect of BIO treatment and PD-MSC co-culturing on endothelial permeability in the CCl_4-treated group ($p < 0.05$) (Fig. 6B).

In contrast to the effect of BIO treatment, endothelial permeability was significantly enhanced by IWP treatment compared with that in the control group ($p < 0.05$) (Fig. 6C). Furthermore, although endothelial permeability was strongly enhanced by co-treatment with IWP and CCl_4 ($p < 0.05$), it was effectively inhibited by PD-MSC co-culturing regardless of IWP or CCl_4 treatment ($p < 0.05$). Furthermore, to investigate whether alteration of endothelial permeability was regulated by PD-MSC co-culture, we inhibited the Wnt pathway by pretreatment of PD-MSCs with IWP before co-culturing with endothelial cells. Interestingly, endothelial permeability was significantly enhanced by co-culturing with IWP-pretreated CP-MSCs compared to control culturing conditions ($p < 0.05$) (Fig. 6C). Taken together, our results suggest that PD-MSC Tx and the *in vitro* co-culture system promote hepatic regeneration in the CCl_4-injured liver by regulating the vascular structure and endothelial permeability through the Wnt signaling pathway.

Discussion

In the present study, we demonstrated that PD-MSC Tx contributed to liver regeneration in a cirrhotic rat model *via* restoration of vascular structure and function with expression of multiple angiogenic factors. In addition, these effects were found to depend on increased expression of β-catenin and p-LRP6. In liver diseases, SECs play a key role in hepatic regeneration by changing their structure and function. A previous study showed that lung-derived MSCs induce angiogenesis by stimulating β-catenin through interleukin-1β and NF-κB [28], and MSCs were found to have a vascular remodeling effect by secreting exosomes and improving neovascularization [29, 30]. The architecture of hepatic vasculature in the cirrhotic liver is characterized by distorted vessels of varying diameters that perfuse nodules of parenchymal cells, and SECs lose their fenestrations and develop a deficiency of vasodilator molecules [31, 32].

Recently, Hu J et al. demonstrated that angiocrine factors released from the sinusoidal endothelium are required for liver regeneration [33]. In our data, engrafted PD-MSCs were found in tissues surrounding the hepatic vein with increased vWF expression, and vascular tube formation was significantly recovered by PD-MSC co-culturing (Fig. 1A and 2C). Furthermore, PD-MSC Tx enhanced hepatic regeneration with vessel recovery by elevating protein levels related to hepatic function and angiogenesis (Fig. 1E-F and 2A-E).

During liver regeneration, hepatic vessels play a major role in hepatic regeneration [34]. Upregulating chemokine receptors and cytokines, such as CXCR7 and IL-6, induces the activation of endothelial cells, which modulate liver regeneration and fibrosis through VEGF [35]. Furthermore, VEGFR2-Id1-mediated pro-angiogenic factors in LSECs were shown to promote hepatic proliferation and HGF expression by stabilizing HIF-1α [36]. We therefore explored the effect of PD-MSC Tx on the relationship between endothelial activation and hepatocyte proliferation in an *ex vivo* co-culture model (Fig. 2C). PD-MSC Tx induced an increase in the expression of angiogenic factors including vWF, Endoglin, VEGF, and VE-cadherin, which are important for regulating endothelial permeability and assembly of new blood vessels (Fig. 2A-B and 2D-E). PD-MSC-induced VEGF stimulation may affect cell-cell adhesion by activating VE-cadherin and β-catenin, which was previously shown to be an important step in modulating intercellular contacts during angiogenesis and in regulating vascular permeability [8].

Wnt/β-catenin signaling plays important roles in endothelial proliferation, migration and survival and can modulate vascular remodeling [5, 19]. This signaling pathway is initiated by Wnt binding to Frizzled (Fz)/low-density lipoprotein receptor-related proteins 5 and 6 (LRP5 and LRP6) and is mediated by the transcriptional activity of β-catenin. Stabilized cytoplasmic β-catenin then translocates to the nucleus and regulates target gene expression [5, 6]. Moreover, Fz and LRP5/6 receptors are critical upstream regulators of the Wnt/β-catenin signaling cascade in the vascular system [10]. Our results showed that decreased protein levels of LRP6 and β-catenin in the injured liver model were effectively recovered after PD-MSC Tx and that increased β-catenin expression was localized with vWF in the nucleus of hepatic endothelial cells (Fig. 3B-D). We also found that the expression levels of LRP6, β-catenin, Axin2, c-Myc, and cyclin D1 were decreased in human cirrhotic liver tissues (Fig. 4A-B and 4D-F). In addition to its transcriptional function, β-catenin also participates in the cell-cell adhesion process involved in controlling vascular permeability [8]. Endothelial permeability is rapidly regulated through cadherin molecules, such as VE-cadherin and N-cadherin, at sites of cell-cell adherens junctions [9]. Cytoplasmic catenins are essential for cadherin-mediated cell adhesion [35, 36].

Furthermore, the importance of the interaction between β-catenin and adhesion proteins in vascular permeability has been demonstrated using a genetic mouse model of integrin-associated focal adhesion tyrosine kinase (FAK) inhibition. FAK inhibition in endothelial cells prevents β-catenin dissociation and endothelial barrier breakdown by VEGF and Src tyrosine kinase [37]. Regardless of the importance of Wnt/β-catenin signaling for endothelial function and permeability, the mechanism by which this system elicits its pro-angiogenic effect is poorly understood. As such, the role of the Wnt system has been limited to only facilitating hepatic proliferation during liver regeneration [38]. Recently, MSCs were shown to significantly reduce endothelial permeability in co-cultured HUVECs following exposure to VEGF, which enhances the VE-cadherin/β-catenin interaction [19]. This result was different from our data but partially consistent with our findings that MSCs reduced HUVEC permeability in our *in vitro* co-culture system. We observed that co-culturing PD-MSCs with HUVECs decreased endothelial permeability by increasing β-catenin expression and stimulating its nuclear translocation (Fig. 6B and C). Consistent with our data, previous studies showed that human umbilical cord MSCs (hucMSCs) stimulate β-catenin nuclear translocation and endothelial cell activation [30]. However, excessive activation of liver vessels was

shown to result in liver cirrhosis and hypertension by regulating monocyte recruitment and infiltration *via* VEGF [39]. PD-MSC Tx was shown to stimulate the expression of markers related to angiogenic and β-catenin signaling factors *in vivo* (Fig. 2A-B, 2D-E, and 3C-D). The *in vitro* effect of PD-MSCs on endothelial permeability was also found to be β-catenin-dependent (Fig. 6B-C). These results imply that Wnt/β-catenin may be key molecules during PD-MSC Tx-induced liver regeneration by regulating pro-regenerative factors and endothelial permeability. However, we need to further investigate the correlation between permeability and angiogenesis of endothelial cells in liver regeneration.

Conclusions

In a CCl_4-injured rat model, PD-MSCs regulate functional vascular remodeling *via* HIF-1α-mediated activation of pro-angiogenic factors. In addition, PD-MSCs regulate the permeability of damaged endothelial cells through Wnt signaling mediated by β-catenin and regulate liver regeneration by increasing hepatocyte proliferation (Fig. 7). Our findings reveal new mechanisms and a potential target for stimulating the processes of liver regeneration involved in vascular remodeling and help us to understand stem cell-based therapeutic mechanisms.

Abbreviations

PD-MSCs, placenta-derived mesenchymal stem cells; CCl_4, Carbon tetrachloride; LSECs, liver sinusoidal endothelial cells; EC, endothelial cell; VEGF, vascular endothelial growth factor; HGF, hepatocyte growth factor; MMP, matrix metalloproteinases; NTx, non-transplantation; Tx, transplantation.

Declarations

Author Contributions:

JHC did analysis and interpretation of data, and manuscript drafting. JHJ did analysis and collection of data. GDK, EJ, SKB, and SHB helped critical discussion. GJK conceived and designed the experiments, and directed manuscript drafting, financial support, and final approval of manuscript. All authors read and approved the final manuscript.

Funding:

This work was supported by the Korea Health Technology R&D Project through the Korea health Industry Development Institute (KHIDI), funded by the Ministry of Health & Welfare, Republish of Korea (HI17C1050), by Basic Science Research Program through the National Research Foundation of Korea (NRF) funded by the Ministry of Education, Science and Technology (2020M3A9B3026182) and This research was supported by a grant from Ministry of Food and Drug Safety in 2021 (18172MFDS182).

Availability of data and materials:

All data analyzed for this study are included in this article.

Ethics approval and consent to participate:

Human liver specimen. Human liver tissues from normal and cirrhotic patients were provided by Yonsei University, Wonju College of Medicine (Korea-21 Cirrhosis Project).

CCl_4-injured rat liver model. All animal experimental processes were conducted using protocols according to the Institutional Review Board of CHA General Hospital, Seongnam, Korea (IACUC-130009).

Cell culture. Placenta collection and their use for research were approved by the Institutional Review Board of CHA General Hospital, Seoul, Korea (IRB #07-18).

Consent for publication:

Not applicable.

Conflict of interest:

The authors declare no conflict of interest.

References

1. Natarajan V, Harris EN, Kidambi S. SECs (Sinusoidal Endothelial Cells), Liver Microenvironment, and Fibrosis. Biomed Res Int. 2017;2017:4097205.
2. Hu J, Srivastava K, Wieland M, Runge A, Mogler C, Besemfelder E, et al. Endothelial cell-derived angiopoietin-2 controls liver regeneration as a spatiotemporal rheostat. Science. 2014;343(6169):416-9.
3. Wang WL, Zheng XL, Li QS, Liu WY, Hu LS, Sha HC, et al. The effect of aging on VEGF/VEGFR2 signal pathway genes expression in rat liver sinusoidal endothelial cell. Mol Cell Biochem. 2021;476(1):269-77.
4. Rodriguez-Vilarrupla A, Lavina B, Garcia-Caldero H, Russo L, Rosado E, Roglans N, et al. PPARalpha activation improves endothelial dysfunction and reduces fibrosis and portal pressure in cirrhotic rats. J Hepatol. 2012;56(5):1033-9.
5. Zhao L, Jin Y, Donahue K, Tsui M, Fish M, Logan CY, et al. Tissue Repair in the Mouse Liver Following Acute Carbon Tetrachloride Depends on Injury-Induced Wnt/beta-Catenin Signaling. Hepatology. 2019;69(6):2623-35.
6. Pradhan-Sundd T, Kosar K, Saggi H, Zhang R, Vats R, Cornuet P, et al. Wnt/beta-Catenin Signaling Plays a Protective Role in the Mdr2 Knockout Murine Model of Cholestatic Liver Disease. Hepatology. 2020;71(5):1732-49.
7. Doring Y, Noels H, van der Vorst EPC, Neideck C, Egea V, Drechsler M, et al. Vascular CXCR4 Limits Atherosclerosis by Maintaining Arterial Integrity: Evidence From Mouse and Human Studies.

Circulation. 2017;136(4):388-403.
8. Gavard J. Endothelial permeability and VE-cadherin: a wacky comradeship. Cell Adh Migr. 2014;8(2):158-64.
9. Birdsey GM, Shah AV, Dufton N, Reynolds LE, Osuna Almagro L, Yang Y, et al. The endothelial transcription factor ERG promotes vascular stability and growth through Wnt/beta-catenin signaling. Dev Cell. 2015;32(1):82-96.
10. Alapati D, Rong M, Chen S, Lin C, Li Y, Wu S. Inhibition of LRP5/6-mediated Wnt/beta-catenin signaling by Mesd attenuates hyperoxia-induced pulmonary hypertension in neonatal rats. Pediatr Res. 2013;73(6):719-25.
11. Nagaraj AB, Joseph P, Kovalenko O, Singh S, Armstrong A, Redline R, et al. Critical role of Wnt/beta-catenin signaling in driving epithelial ovarian cancer platinum resistance. Oncotarget. 2015;6(27):23720-34.
12. Vitali I, Fievre S, Telley L, Oberst P, Bariselli S, Frangeul L, et al. Progenitor Hyperpolarization Regulates the Sequential Generation of Neuronal Subtypes in the Developing Neocortex. Cell. 2018;174(5):1264-76 e15.
13. Deb A. Cell-cell interaction in the heart via Wnt/beta-catenin pathway after cardiac injury. Cardiovasc Res. 2014;102(2):214-23.
14. Li W, Zhu C, Li Y, Wu Q, Gao R. Mest attenuates CCl4-induced liver fibrosis in rats by inhibiting the Wnt/beta-catenin signaling pathway. Gut Liver. 2014;8(3):282-91.
15. Lee CW, Chen YF, Wu HH, Lee OK. Historical Perspectives and Advances in Mesenchymal Stem Cell Research for the Treatment of Liver Diseases. Gastroenterology. 2018;154(1):46-56.
16. Karp JM, Leng Teo GS. Mesenchymal stem cell homing: the devil is in the details. Cell Stem Cell. 2009;4(3):206-16.
17. Saleh FA, Whyte M, Genever PG. Effects of endothelial cells on human mesenchymal stem cell activity in a three-dimensional in vitro model. Eur Cell Mater. 2011;22:242-57; discussion 57.
18. Pati S, Gerber MH, Menge TD, Wataha KA, Zhao Y, Baumgartner JA, et al. Bone marrow derived mesenchymal stem cells inhibit inflammation and preserve vascular endothelial integrity in the lungs after hemorrhagic shock. PLoS One. 2011;6(9):e25171.
19. Pati S, Khakoo AY, Zhao J, Jimenez F, Gerber MH, Harting M, et al. Human mesenchymal stem cells inhibit vascular permeability by modulating vascular endothelial cadherin/beta-catenin signaling. Stem Cells Dev. 2011;20(1):89-101.
20. Jung J, Choi JH, Lee Y, Park JW, Oh IH, Hwang SG, et al. Human placenta-derived mesenchymal stem cells promote hepatic regeneration in CCl4 -injured rat liver model via increased autophagic mechanism. Stem Cells. 2013;31(8):1584-96.
21. Lee MJ, Jung J, Na KH, Moon JS, Lee HJ, Kim JH, et al. Anti-fibrotic effect of chorionic plate-derived mesenchymal stem cells isolated from human placenta in a rat model of CCl(4)-injured liver: potential application to the treatment of hepatic diseases. J Cell Biochem. 2010;111(6):1453-63.

22. Choi JH, Lim SM, Yoo YI, Jung J, Park JW, Kim GJ. Microenvironmental Interaction Between Hypoxia and Endothelial Cells Controls the Migration Ability of Placenta-Derived Mesenchymal Stem Cells via alpha4 Integrin and Rho Signaling. J Cell Biochem. 2016;117(5):1145-57.
23. Berzigotti A. Advances and challenges in cirrhosis and portal hypertension. BMC Med. 2017;15(1):200.
24. Qi X, He C, Guo W, Yin Z, Wang J, Wang Z, et al. Transjugular intrahepatic portosystemic shunt for portal vein thrombosis with variceal bleeding in liver cirrhosis: outcomes and predictors in a prospective cohort study. Liver Int. 2016;36(5):667-76.
25. Vestweber D. VE-cadherin: the major endothelial adhesion molecule controlling cellular junctions and blood vessel formation. Arterioscler Thromb Vasc Biol. 2008;28(2):223-32.
26. Liu B, Zhou H, Zhang T, Gao X, Tao B, Xing H, et al. Loss of endothelial glucocorticoid receptor promotes angiogenesis via upregulation of Wnt/beta-catenin pathway. Angiogenesis. 2021;24(3):631-45.
27. Jho EH, Zhang T, Domon C, Joo CK, Freund JN, Costantini F. Wnt/beta-catenin/Tcf signaling induces the transcription of Axin2, a negative regulator of the signaling pathway. Mol Cell Biol. 2002;22(4):1172-83.
28. Sun J, Chen J, Cao J, Li T, Zhuang S, Jiang X. IL-1beta-stimulated beta-catenin up-regulation promotes angiogenesis in human lung-derived mesenchymal stromal cells through a NF-kappaB-dependent microRNA-433 induction. Oncotarget. 2016;7(37):59429-40.
29. Ma J, Zhao Y, Sun L, Sun X, Zhao X, Sun X, et al. Exosomes Derived from Akt-Modified Human Umbilical Cord Mesenchymal Stem Cells Improve Cardiac Regeneration and Promote Angiogenesis via Activating Platelet-Derived Growth Factor D. Stem Cells Transl Med. 2017;6(1):51-9.
30. Zhang B, Wu X, Zhang X, Sun Y, Yan Y, Shi H, et al. Human umbilical cord mesenchymal stem cell exosomes enhance angiogenesis through the Wnt4/beta-catenin pathway. Stem Cells Transl Med. 2015;4(5):513-22.
31. Poisson J, Lemoinne S, Boulanger C, Durand F, Moreau R, Valla D, et al. Liver sinusoidal endothelial cells: Physiology and role in liver diseases. J Hepatol. 2017;66(1):212-27.
32. Xie G, Wang X, Wang L, Wang L, Atkinson RD, Kanel GC, et al. Role of differentiation of liver sinusoidal endothelial cells in progression and regression of hepatic fibrosis in rats. Gastroenterology. 2012;142(4):918-27 e6.
33. Uda Y, Hirano T, Son G, Iimuro Y, Uyama N, Yamanaka J, et al. Angiogenesis is crucial for liver regeneration after partial hepatectomy. Surgery. 2013;153(1):70-7.
34. Ding BS, Cao Z, Lis R, Nolan DJ, Guo P, Simons M, et al. Divergent angiocrine signals from vascular niche balance liver regeneration and fibrosis. Nature. 2014;505(7481):97-102.
35. Heuberger J, Birchmeier W. Interplay of cadherin-mediated cell adhesion and canonical Wnt signaling. Cold Spring Harb Perspect Biol. 2010;2(2):a002915.
36. Shashikanth N, Petrova YI, Park S, Chekan J, Maiden S, Spano M, et al. Allosteric Regulation of E-Cadherin Adhesion. J Biol Chem. 2015;290(35):21749-61.

37. Chen XL, Nam JO, Jean C, Lawson C, Walsh CT, Goka E, et al. VEGF-induced vascular permeability is mediated by FAK. Dev Cell. 2012;22(1):146-57.
38. Yang J, Mowry LE, Nejak-Bowen KN, Okabe H, Diegel CR, Lang RA, et al. beta-catenin signaling in murine liver zonation and regeneration: a Wnt-Wnt situation! Hepatology. 2014;60(3):964-76.
39. Yang L, Kwon J, Popov Y, Gajdos GB, Ordog T, Brekken RA, et al. Vascular endothelial growth factor promotes fibrosis resolution and repair in mice. Gastroenterology. 2014;146(5):1339-50 e1.

Figure

Figure 7 is not available with this version.

Supplementary Figures

Supplementary Figures are not available with this version.

Figures

Figure 1. Choi and Jun et al.,

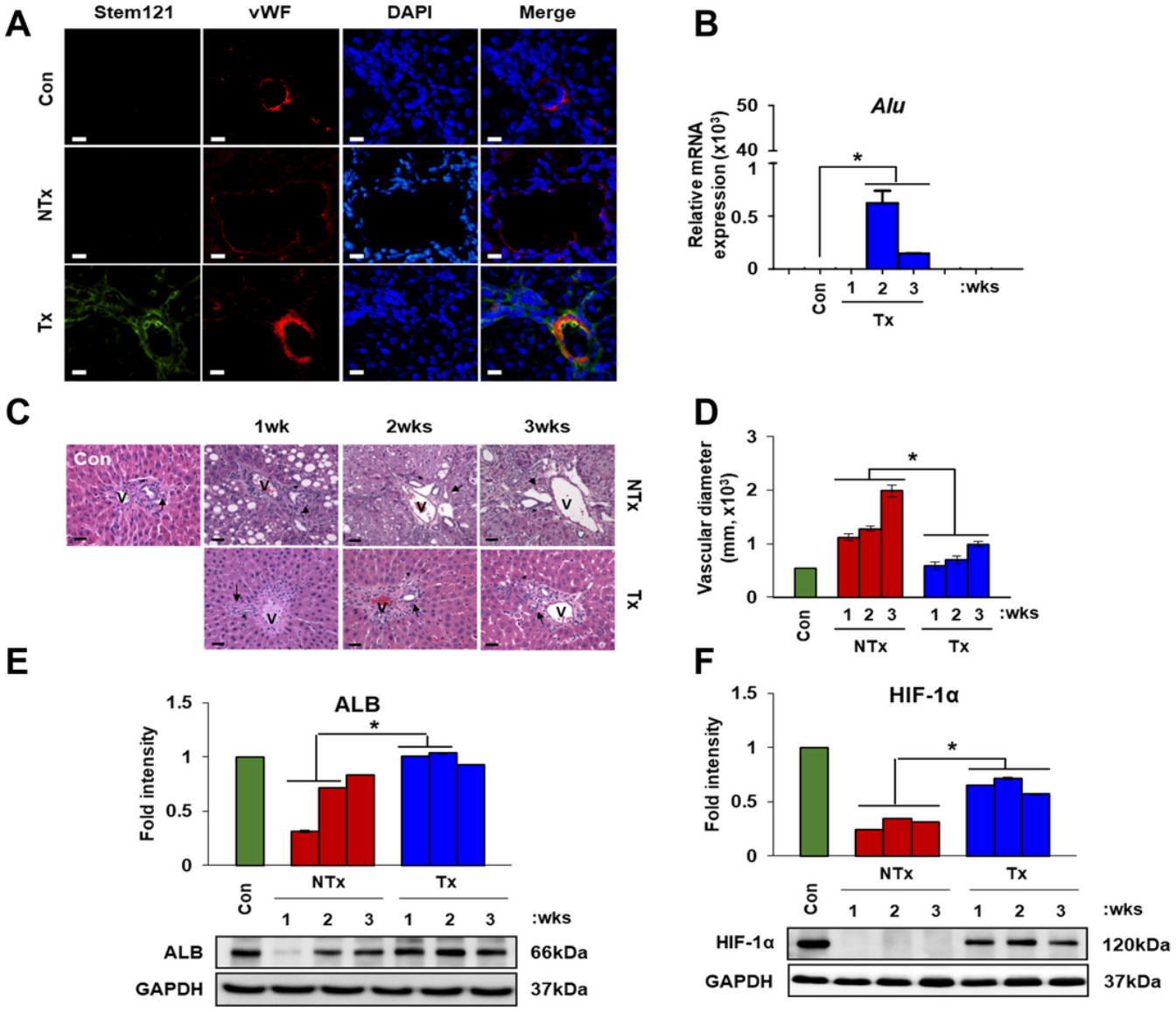

Figure 1

Engrafted PD-MSC decreases the hepatic vein diameter and improves the liver regeneration in the CCl4-injured rat model. A Stem121 (human cytoplasm-specific antibody) and vWF expression in liver tissues at 1 week were detected by double immunofluorescence in Con, NTx, and Tx livers. Scale bar: 80 μm. B mRNA levels of human Alu were determined in all liver tissues by real-time PCR. Bar graph shows the relative expression level of Alu at 1, 2 and 3 weeks of the Tx group and Con group. Equal amounts of RNA from rats at 1, 2 and 3 weeks were pooled. Rat GAPDH was used as an internal control. All experiments were performed in triplicate. C H&E staining of livers at 1, 2 and 3 weeks after PD-MSC Tx and NTx in CCl4 rats. Serial sections of liver tissues from Con (n=5), CCl4 (n=5), NTx (n=5) and PD-MSC Tx (n=5) rats were

obtained. Scale bar: 100 μm. D Quantification of the hepatic vein diameter at 1, 2 and 3 weeks after PD-MSC Tx in CCl4 rats. Protein expression levels of E ALB (hepatocyte functional marker) and F HIF-1α in liver tissue from a CCl4 rat after PD-MSC Tx were detected by Western blot analysis. All experiments were performed in triplicate. Data are expressed as the mean ± SD of triplicate reactions. $p<0.05$. Control, Con; CCl4-injured, CCl4; non-transplantation, NTx; PD-MSC transplantation, Tx; weeks, wks.

Figure 2. Choi and Jun et al.,

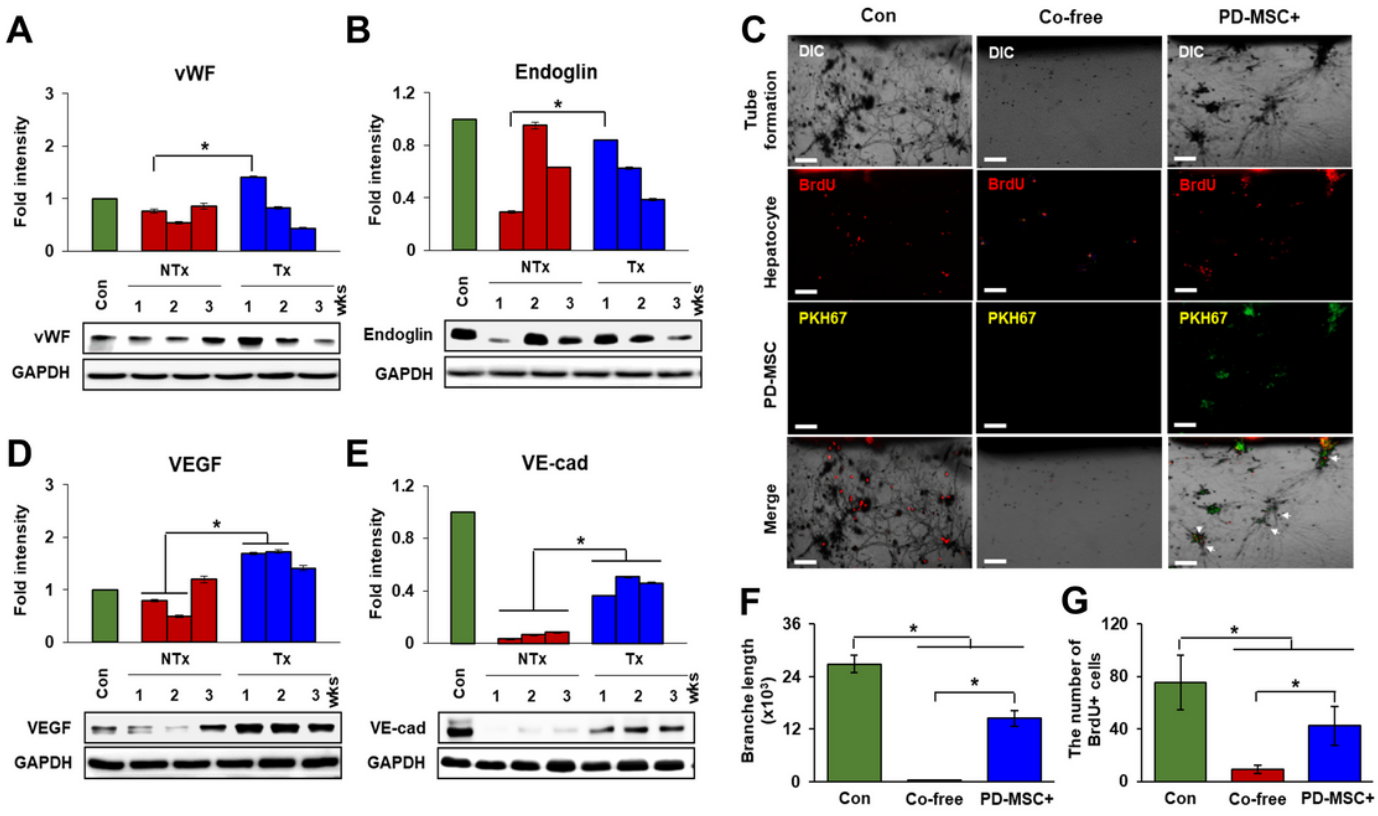

Figure 2

Transplanted PD-MSCs stimulate angiogenesis and hepatocyte proliferation in vivo and ex vivo. Protein expression of markers related to angiogenesis, such as A vWF, B endoglin, D VEGF and E VE-cadherin, in CCl4 rat model after PD-MSC Tx were analyzed by Western blot. Equal amounts of protein from individual animals at 1, 2 and 3 weeks were pooled and resolved SDS-PAGE. Signal intensities on the blots were quantified by densitometry. GAPDH was used as a loading control. C Tube formation of the rat aortic ring and proliferation of WB-F344 cells co-cultured with PD-MSC were analyzed by a modified rat aortic ring assay. Extracted rat aortic rings and WB-F344 cells were co-cultured with PD-MSC after 24-hour CCl4 (3 mM) treatment. Scale bar: 100 μm. Arrow heads indicate BrdU-positive WB-F344 cells. F Quantification of branch length and G BrdU-positive hepatocytes in the rat aortic ring assay. Data are expressed as the mean ± SD. All experiments were performed in triplicate. $p<0.05$. non-transplantation, NTx; PD-MSC transplantation, Tx; without PD-MSC co-culture, Co-free; with PD-MSC co-culture, PD-MSC +.

Figure 3. Choi and Jun et al.,

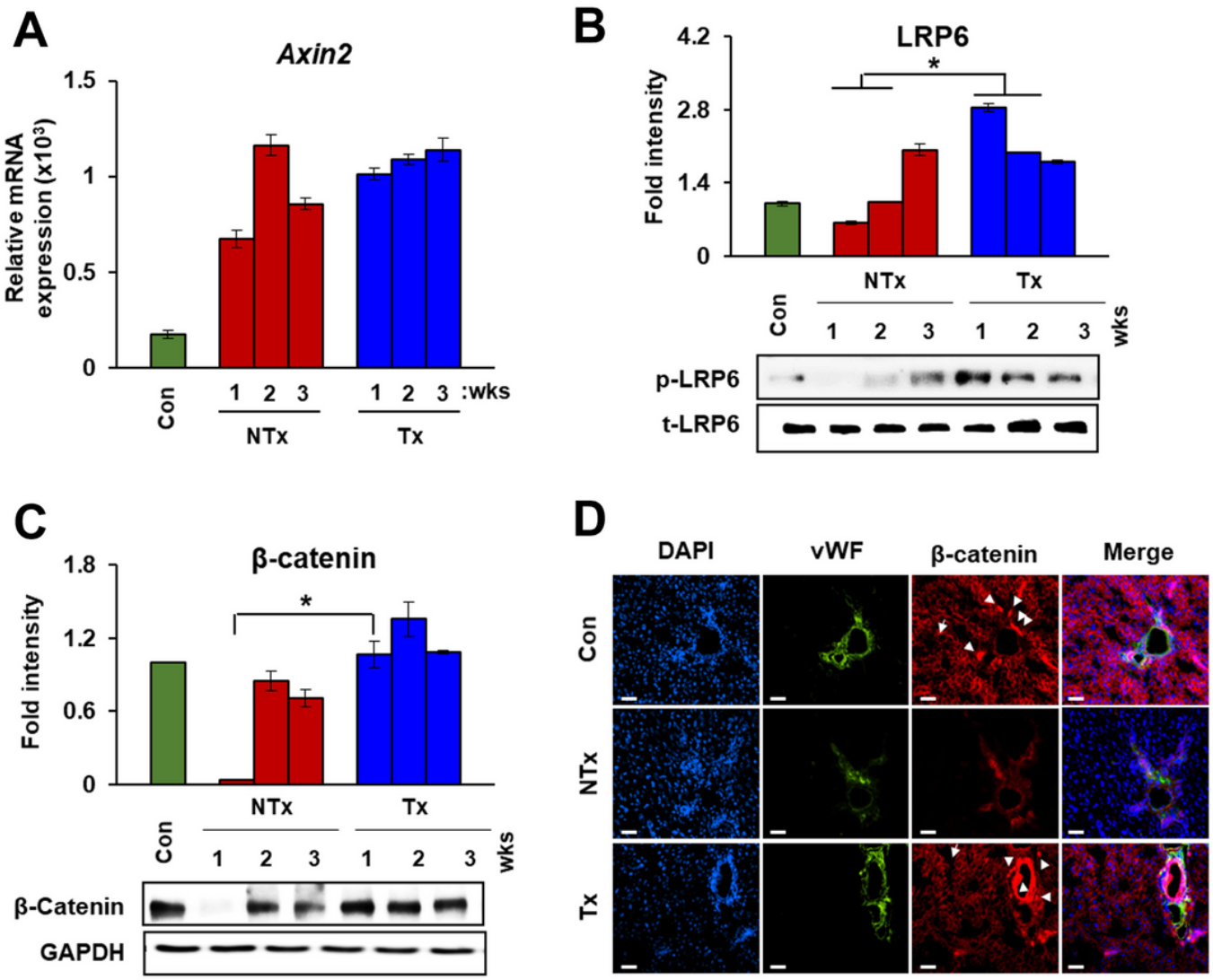

Figure 3

PD-MSCs promote hepatic regeneration through Wnt signaling in the CCl4-injured rat model. A Axin2 mRNA levels in total liver tissues were determined by real-time PCR. Equal amounts of RNA from animals at 1, 2 and 3 weeks were pooled. Rat GAPDH primers were used as an internal control. Protein expression levels of B LRP6 and C active β-catenin in liver tissue of a CCl4 rat after PD-MSC Tx were analyzed by Western blot. Equal amounts of protein from animals at 1, 2 and 3 weeks were pooled and resolved by SDS-PAGE. Signal intensities on the blots were quantified by densitometry. GAPDH was used as a loading control. D Expression levels of vWF and β-catenin were detected by double immunofluorescence of liver tissues from control, NTx and Tx groups in the CCl4-injured rat model at 1 week. Scale bar: 80 μm. Arrow heads indicate double-positive staining of β-catenin and vWF in endothelial cells in liver tissues. All

experiments were performed in triplicate. Data are expressed as the mean ± SD. p<0.05. Control, Con; CCl4-injured, CCl4; non-transplantation, NTx; PD-MSC transplantation, Tx.

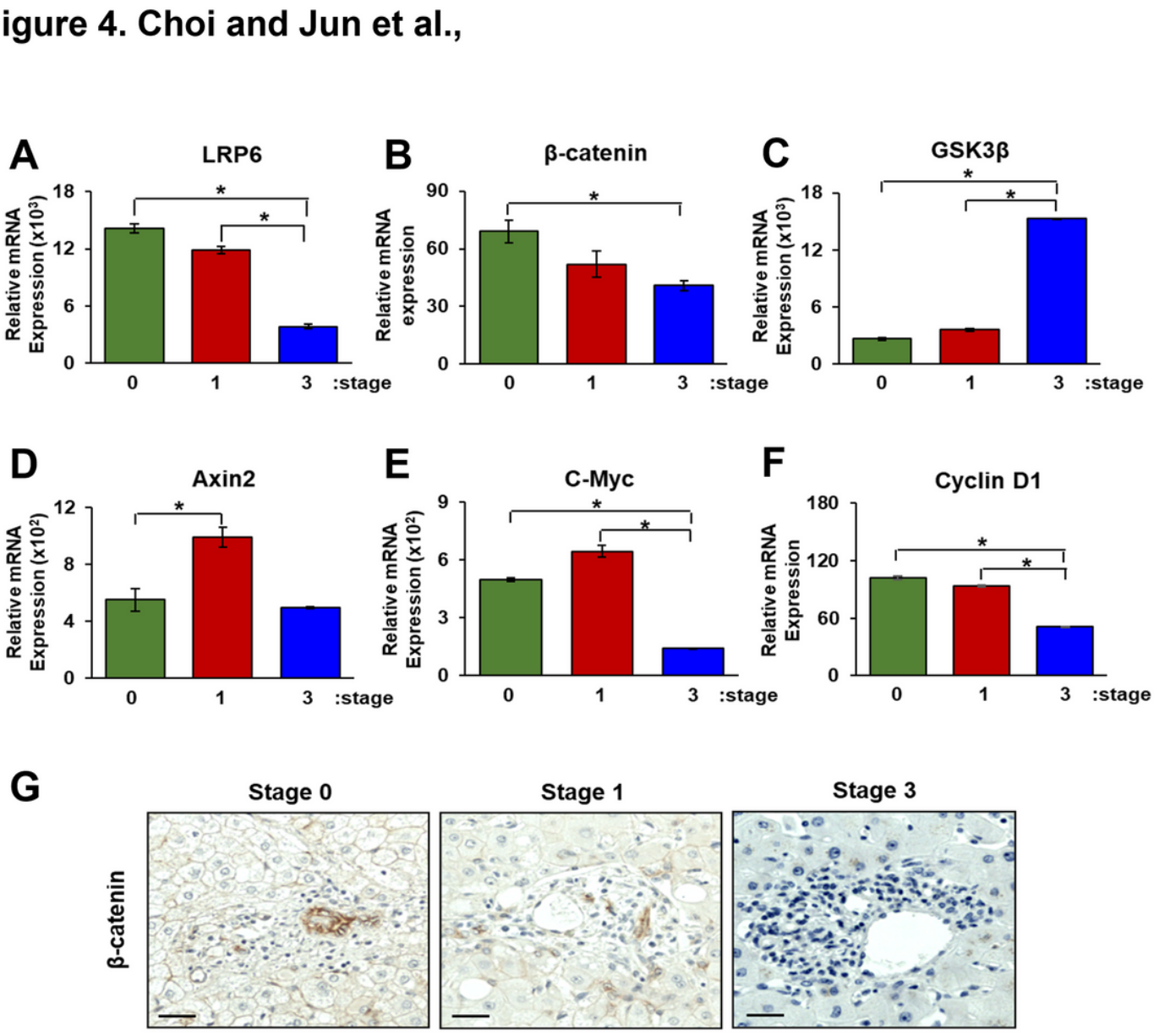

Figure 4

Expression of Wnt signaling genes in endothelial cells correlates with liver cirrhosis in human liver. mRNA expression levels of Wnt signaling markers, A LRP6, B β-catenin, C GSK3β, D Axin2, E c-Myc and F cyclin D1, at different developmental stages were determined by real-time PCR. Equal amounts of RNA from liver tissues at each stage (n=5) were pooled. Human 18S rRNA was used as an internal control. G β-Catenin localization was detected in the outer layer of the hepatic vein (SECs) in human liver tissues by immunohistochemistry. Scale bar: 70 μm. All experiments were performed in triplicate. Data are expressed as the mean ± SD. p<0.05.

Figure 5. Choi and Jun et al.,

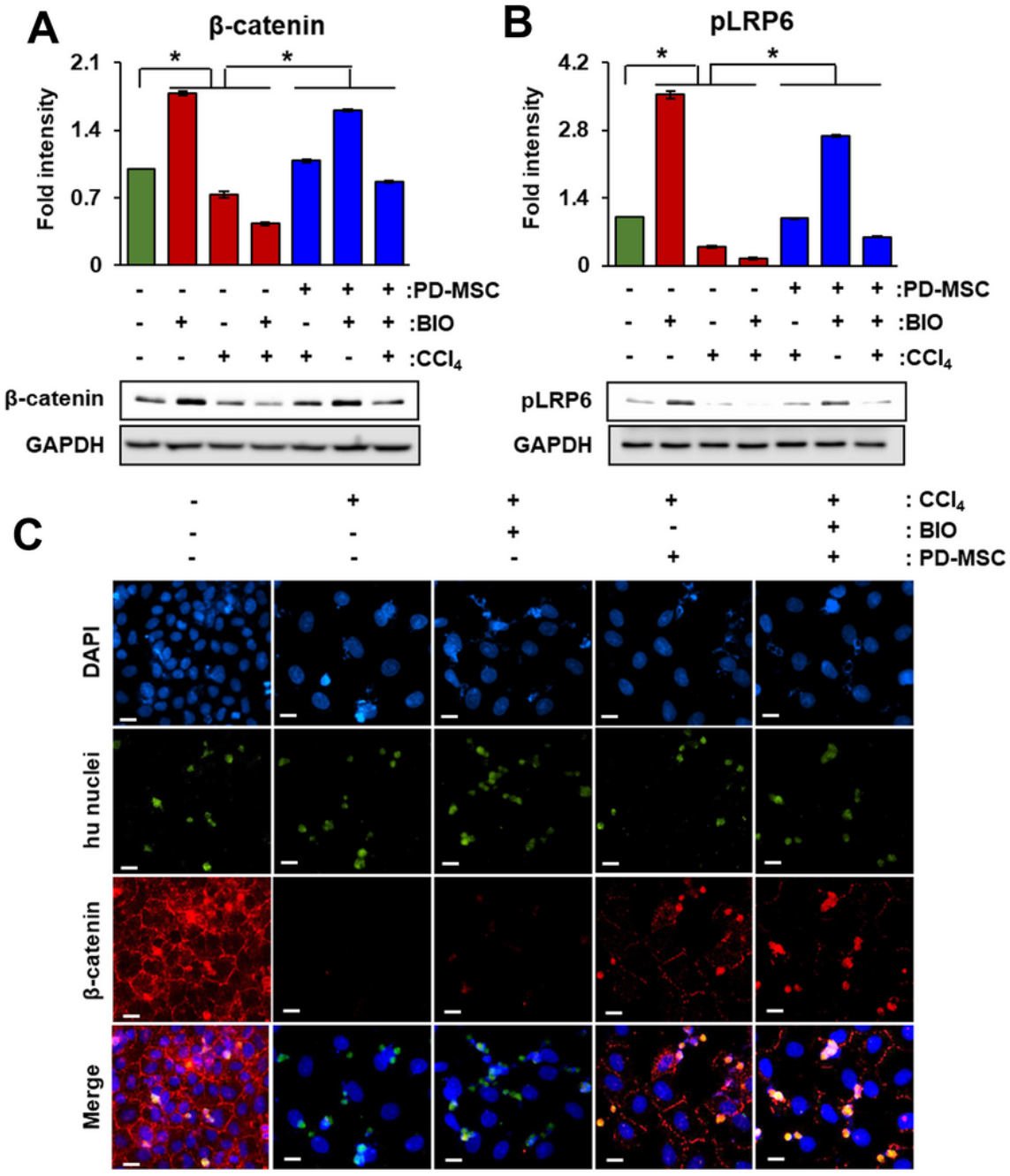

Figure 5

PD-MSCs stimulate the expression of markers related to Wnt signaling in HUVECs. Protein expression levels of A active β-catenin and B p-LRP6 in HUVECs co-cultured with WB-F344 cells and PD-MSC after treatment with or without CCl4 (3 mM) or BIO (10 nM) were detected by Western blot analysis. Equal amounts of protein from cultured cells were pooled and resolved by SDS-PAGE. Signal intensities on the blots were quantified by densitometry. GAPDH was used as a loading control. All experiments were

performed in triplicate. Data are expressed as the mean ± SD. p<0.05. C Localization of human nuclei and active β-catenin in HUVECs were analyzed by double immunofluorescence. Scale bar=70 μm. PD-MSC co-culture, PD-MSC; BIO-treated, BIO; CCl4-treated, CCl4.

Figure 6. Choi and Jun et al.,

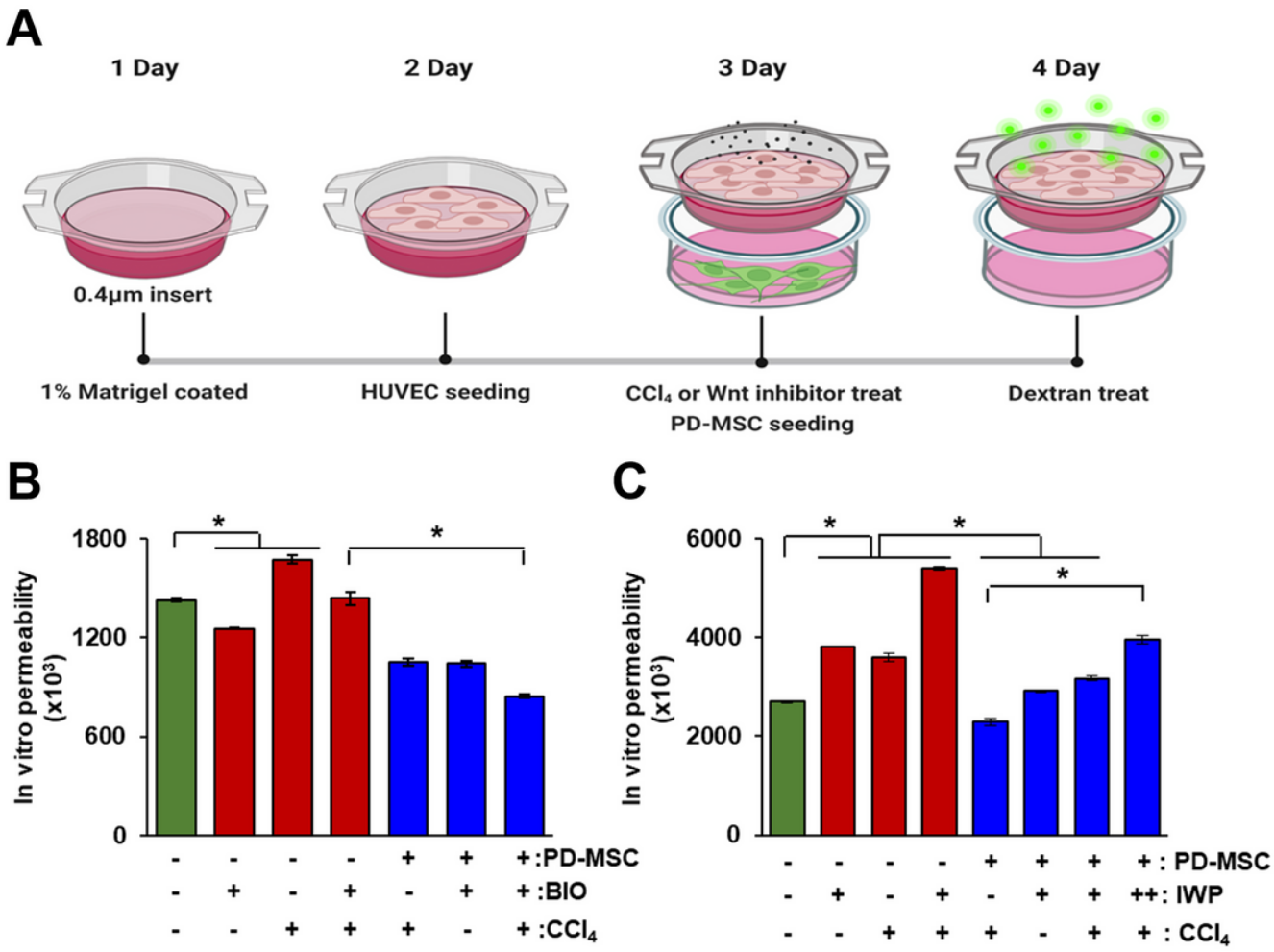

Figure 6

PD-MSCs decrease HUVEC permeability through Wnt signaling in vitro. A Effect of PD-MSC on HUVEC permeability was analyzed by an endothelial permeability assay. HUVECs were seeded at 80% confluence into upper transwell chambers pre-coated with 1% Matrigel. After culturing, HUVECs were treated with CCl4 or BIO and then co-cultured with PD-MSC for 24 hours. FITC-dextran was added to the upper chambers after 30 minutes. Supernatants in the lower chambers were harvested, and the passage of dextran into the lower chambers of samples treated with B BIO or C IWP were detected by luminescence. Data are expressed as the mean ± SD. PD-MSC culture, PD-MSC; BIO-treated, BIO; CCl4-treated, CCl4; IWP-treated, IWP.

Supplementary Files

This is a list of supplementary files associated with this preprint. Click to download.

- SCRTGraphicalabstractChoietal..tif